Geology, Geophysics & Environment 2025, vol. 51 (1): 27–42

A three-component model of kerogen kinetics on the example of the Menilite Beds

Tomasz Słoczyński[1], Irena Matyasik[2], Karol Spunda[3]

[1] *Oil and Gas Institute – National Research Institute, Krakow, Poland, ORCID ID: 0000-0002-6355-2916*
[2] *Oil and Gas Institute – National Research Institute, Krakow, Poland, ORCID ID: 0000-0003-3696-9772*
[3] *Oil and Gas Institute – National Research Institute, Krakow, Poland, e-mail: spunda@inig.pl (corresponding author), ORCID ID: 0000-0001-7392-5715*

Received: 20 May 2024; accepted: 14 January 2025; first published online: 25 March 2025

Abstract: This paper presents the concept of constructing three-component kinetic models of kerogen. The method was developed based on the kinetic mass model constructed from Rock-Eval pyrolysis and Py-GC analysis results. The parameters of the discrete function describing the distribution of activation energy (E_a) and the constant values of the reaction rate (A) for the mass model were optimized based on the results of Rock-Eval pyrolysis in the Kinetics15 program. With aid of multistage isothermal pyrolysis of Py-GC performed for the same duration at different temperatures, the percentages of each hydrocarbon fraction obtained during the successive stages of pyrolysis were determined. The determined fractions were assigned an appropriate (resulting from the mass model) value of activation energy.

The multi-component kinetic model of kerogen constructed in this way enabled the calculation of the shares of individual hydrocarbon fractions generated at different stages of thermal transformation of the source rocks. Simulations of the composition of generated hydrocarbons for the developed model were carried out in the PetroMod Kinetic Editor. The results of the simulation justified the creation of multi-component kinetic models for each of the potential source formations located in the study area. Their implementation into the petroleum system model makes it possible to not only forecast the total amount of generated hydrocarbons but also the dynamics of the generation process and the shares of the generated fractions at various stages of thermal transformation of the source rocks.

The research material consisted of Menilite source rocks samples, which are considered to be the main source of hydrocarbon accumulations in the Outer Carpathians.

Keywords: activation energy, kerogen kinetic, three-component kinetic, petroleum system modeling, Rock-Eval, Py-GC, Menilite Beds

INTRODUCTION

The Menilite Beds are considered to be one of the primary source rocks for hydrocarbon accumulations in the Outer Carpathians. The development and application of a three-component kinetic model in modeling the Carpathian petroleum system will enable a more comprehensive analysis, allowing for the modeling of both the dynamics and the efficiency of the hydrocarbon generation process. Unlike single-component models, the three-component models also allows for predictions regarding the proportion of individual hydrocarbon fractions.

One of the fundamental problems in petroleum prospecting, in addition to the prediction of prospective zones, is the quantitative and qualitative estimation of the hydrocarbon generation process. Numerical models, whose task is to reconstruct the most probable scenarios of evolution of the petroleum system leading to hydrocarbon accumulations, require the provision of a broad set of geological, thermal, and geochemical data, the use of which makes it possible to place in geological time and basin space the processes of hydrocarbon generation, migration and accumulation taking place. The scope and quality of input data implemented into simulation models determine reliability of the constructed models and give adequate results. In this case, it means that the use of a three-component kinetic model of kerogen (instead of a bulk model) not only allows for the reconstruction of the overall dynamics of the generation process but also for each of the separated fractions (Hantschel & Kauerauf 2009, Sowiżdżał et al. 2020, Spunda 2020, Spunda et al. 2021).

The formation of hydrocarbons and their molecular composition is determined among others by the type of kerogen and the temperature, at which the process occurs. Both gaseous and liquid hydrocarbons are produced by thermal cracking of kerogen. Kerogen is not a chemically homogeneous substance but is formed from complex organic compounds, mainly carbon, hydrogen, and oxygen, occurring in different proportions, which leads to process of kerogen cracking (formation of hydrocarbons) over a wide range of temperatures, and variability of kinetics related to formation of individual hydrocarbon fractions (Krevelen 1961). In general, in the initial stages of the thermal transformation of kerogen, at the lowest temperatures, mainly liquid hydrocarbon fractions are generated, and as thermal transformation increases, gaseous hydrocarbons, including mainly methane are produced. In the subsequent stages of thermal transformation, the proportions between the individual fractions can vary significantly (Hunt 1979, Bordenave 1993).

Kerogen kinetic models are fundamental inputs in simulation models, enabling the modeling of the dynamics of hydrocarbon generation and their composition. Mass (bulk, single-component) or multi-component models are used in modeling of petroleum systems. Single-component models of kerogen make it possible to reconstruct dynamics of generation process as the total amount of all generated hydrocarbons. On the other hand, multicomponent models provide the opportunity to quantify individual fractions at any stage of the thermal evolution of the source rocks. This possibility makes it conceivable to have appropriate kinetic models of kerogen (developed for specific source rocks) to obtain the most reliable and accurate results.

Mass models have been developed and described in the literature for kerogens from certain petroleum provinces (e.g. Tegelaar & Noble 1994, Zhou & Littke 1999, Santamaria-Orozco 2000, Lewan & Ruble 2002, Spunda & Słoczyński 2022), two-component (gas-oil) (e.g., Ungerer 1990, Waples et al. 1992, Pepper & Corvi 1995, Behar et al. 1997, Dieckmann et al. 1998, 2000, Abu-Ali et al. 1999, Vandenbroucke et al. 1999), or multicomponent (e.g., Espitalié et al. 1988, Ungerer 1990, Abu-Ali et al. 1999, Vandenbroucke et al. 1999, Baur 2019, Wood 2024). These models are also available to users of computer programs for modeling petroleum systems.

Studies of source rocks in petroleum-bearing basins from around the world show that the source rocks have specific characteristics that not only determine the dynamics of the hydrocarbon generation process, but also their composition. Therefore, the use of multicomponent kinetic models developed for specific source rocks could make it possible to estimate the proportion of each hydrocarbon fraction produced at each stage of the thermal transformation of source rocks and increases the accuracy of the calculations performed.

Samples of potential source rocks, based on the analysis of which kinetic models are developed, should meet two basic criteria: they must have a low degree of thermal transformation and the highest possible content of kerogen.

METHODS

The concept of creating multicomponent kinetic models of kerogen proposed by the authors is based on the integration of research results

obtained from two analytical methods: Rock-Eval and Py-GC (pyrolysis coupled with gas chromatography).

Rock-Eval

The Rock-Eval pyrolysis method (Espitalié et al. 1985), developed by the French Petroleum Institute, was used by the authors to select appropriate research material and to develop a mass kinetic model of kerogen. It is commonly used to assess the hydrocarbon potential of source rocks. The analysis is conducted in two stages: stage I involves pyrolysis in an inert gas atmosphere at temperatures ranging from 300 to 650°C; stage II involves oxidation in an air atmosphere at temperatures between 300 and 850°C. The products – hydrocarbons, carbon dioxide, and carbon monoxide – are quantitatively determined. The analysis results are recorded by appropriate detectors and displayed as curves. Based on these curves, parameters and indicators are calculated to determine the rock's hydrocarbon potential, assess thermal transformation, and estimate the degree of realization of the initial hydrocarbon potential. The details of this method was described by Lafargue et al. (1998).

Measurements made using this method are also used to construct mass (single-component) kinetic models of kerogen thermal transformation.

Py-GC

The Py-GC analysis cycle has been designed to use its results to construct a multi-component kinetic model of kerogen, which was developed on the basis of a mass model.

High-temperature pyrolysis was performed using a Frontier Laboratories multi-channel pyrolyzer (Multi-Shot Pyrolyzer EGA/PY-3030D) coupled to a gas chromatograph (GC-2010 Plus) and equipped with a Shimadzu flame ionization detector (FID). For the chromatographic analysis, an Ultra Alloy-5 capillary column with a length of 30.0 m, inner diameter 0.25 mm, and film thickness 0.25 μm was connected to an FID detector. Helium was used as the carrier gas with a constant flow rate of 1.98 mL/min. A column temperature gradient from 30°C (maintained for 5 minutes) to 360°C (maintained for 2 minutes) with an accrual of 10°C/min, a dispenser temperature of 250°C, a split of 10:1, and an FID detector temperature of 360°C was used (Kania & Janiga 2015).

First, the sample was heated to 300°C for 3 minutes to evaporate free hydrocarbons, which were not included in the total balance because they are a product of kerogen transformations under natural geological conditions. After the evaporation of free hydrocarbons, the sample was subjected to multi-stage pyrolysis. The heating temperature during each stage was kept constant, and in subsequent stages was set to 400, 425, 450, 475, 500, 525, 550, 600, 700, and 800°C. Each stage lasted 1 minute. At 800°C, no products were obtained, so the pyrolysis of the sample was terminated. The products from each pyrolysis step were collected using a cryogenic trap and then subjected to chromatographic analysis to determine the proportions of different fractions of hydrocarbons produced: a gaseous fraction consisting of hydrocarbons in the C_1–C_5 range, a liquid fraction in the C_6–C_{14} range, and a heavy hydrocarbon fraction in the C_{15+} range.

RESULTS

Rock-Eval analysis

Six samples from outcrops of the Menilite Beds (Oligocene age) in the Silesian Unit of the Polish Outer Carpathians (Fig. 1) were subjected to preliminary tests to select one for developing a three-component kinetic model of kerogen.

The total organic carbon (TOC) content of the analyzed samples ranges from 3.37% to 8.59% (Table 1), and the hydrocarbon (HC) content, expressed as the sum of parameters S_1 and S_2, is between 6.08 and 46.42 mg HC/g of the rock. The organic matter dispersed in the studied rocks is kerogen II type (Fig. 2). In general, the samples are characterized by a low degree of thermal maturity (T_{max}) and a relatively high hydrocarbon content ($S_1 + S_2$) (Table 1). Sample No. 1, contains 8.29% TOC and hydrogen index (HI) 354 mg HC/g TOC (blue dot in Figure 2) and, characterized by the lowest degree of thermal transformation (T_{max} = 403°C), was selected for the activation energy study.

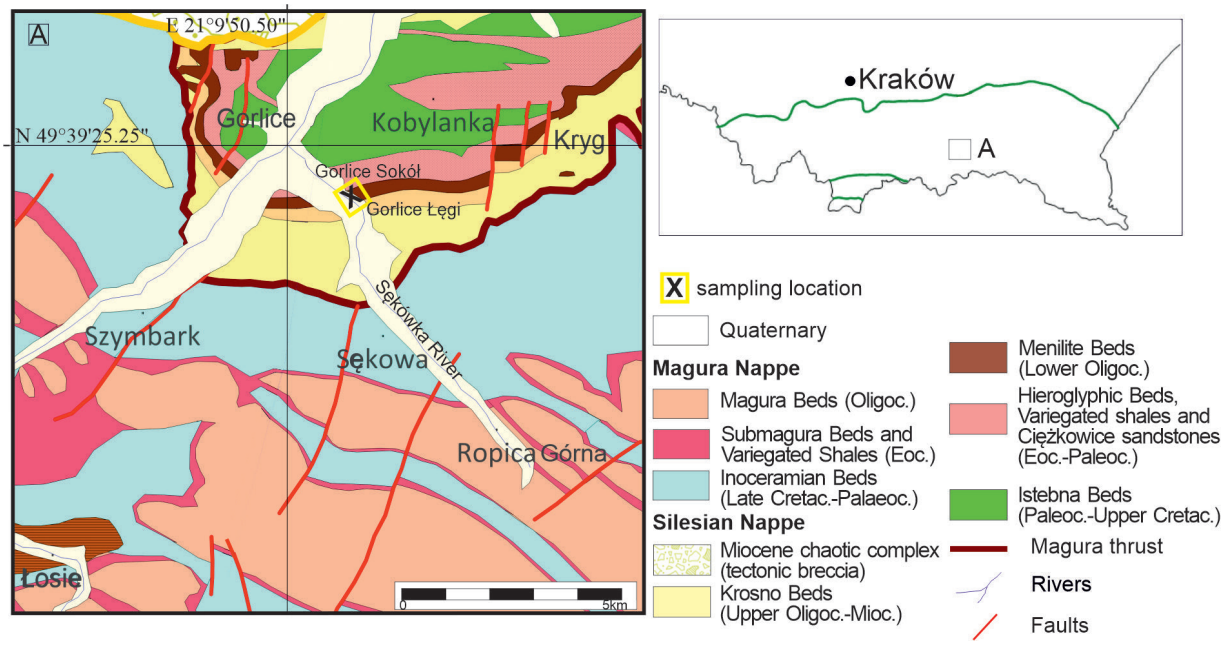

Fig. 1. *Geological map of the study area (after Dziadzio et al. 2016 – modified)*

Table 1
Results of Rock-Eval analysis of the tested samples

Sample	T_{max}	S_1	S_2	S_3	PC	RC	TOC	HI	OI
1	403	0.74	29.37	1.63	2.61	5.68	8.29	354	20
2	416	0.47	35.85	1.12	3.09	2.77	5.86	612	19
3	421	0.09	9.85	0.47	0.87	2.68	3.55	277	13
4	410	0.85	45.57	0.64	3.92	4.67	8.59	531	7
5	409	0.57	23.06	0.6	2.03	4.04	6.07	380	10
6	426	0.04	6.04	1.42	0.58	2.79	3.37	179	42

T_{max} – temperature at which the maximum amount of hydrocarbons is generated during cracking of kerogen [°C]; S_1 – content of free hydrocarbons [mg HC/g rock]; S_2 – amount of hydrocarbons released during cracking of kerogen [mg HC/g rock]; S_3 – amount CO_2 released during cracking of kerogen [mg CO_2/g rock]; PC – pyrolytic carbon content [wt.%.]; RC – residual carbon content [wt.%]; TOC – total organic carbon content [wt.%]; HI – hydrogen index [mg HC/g TOC]; OI – oxygen index [mg CO_2/g TOC].

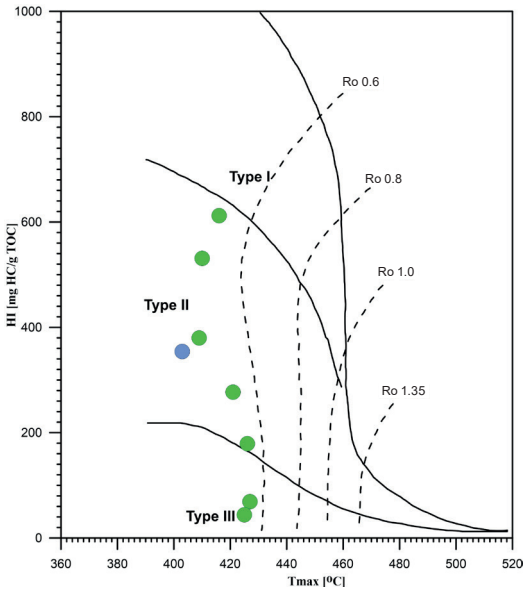

Fig. 2. *HI/T_{max} diagram of organic matter dispersed in the formations of Menilite Beds. Kerogen classification lines according to Espitalié et al. (1984)*

Selecting the sample with the lowest degree of thermal transformation allows for reconstructing the dynamics of kerogen cracking over the widest temperature range.

Additionally, its HI index value is one of the two closest to the average for all samples, making it the most representative in terms of the productivity.

Mass kinetic model of kerogen of Menilite Beds

The construction of kinetic models of kerogen is based on the results of experiments of artificial maturation of kerogen involving its non-isothermal pyrolysis and recording of reaction rate constants at different pyrolysis temperatures, which are carried out in open or closed mode.

To determine the kinetic parameters of the selected sample, it was divided into three parts, and each part was subjected to non-isothermal Rock-Eval pyrolysis with different temperature increments (5, 15, and 25°C/min) in the range of 300 to 650°C. During pyrolysis, the absolute reaction rates (kerogen cracking) were recorded and used to calculate the reaction rate constants k. The results were implemented in the Kinetics15 program, which was used to optimize the discrete activation energy distribution function $f(E_a)$ for a constant reaction rate value A (Spunda & Słoczyński 2022).

The kinetic parameters of kerogen cracking are calculated from the dependence of the reaction rate constant on temperature according to the Arrhenius kinetic equation:

$$k = Ae^{-E_a/RT},$$

which, after transformation, takes the form:

$$E_a = -RT \ln\left(\frac{k}{A}\right),$$

where:

- k – temperature-dependent reaction rate constant [s^{-1}],
- A – constant (Arrhenius) for a given reaction, depending on the type of substrate (type of kerogen) [s^{-1}],
- e – Euler number, the base of the natural logarithm,
- E_a – activation energy [cal/mol],
- R – (universal) gas constant [cal/(mol·K)], $R \approx 1.987$ cal/(mol·K),
- T – temperature [K].

The calculations are performed by mathematical optimizations of the experimental data to determine the activation energy distribution (E_a) for the frequency constant (A) (Sweeney et al. 1987, Burnham & Sweeney 1989, Burnham & Braun 1990, 2017, Hantschel & Kauerauf 2009).

Calculations of the kerogen activation energy distribution were performed using the Kinetics15 software. The method proposed by the authors was to calculate the discrete activation energy distribution with a constant value of the pre-exponential factor A (Arrhenius constant). A graphical visualization with the distribution of activation energy and the value of the constant A is shown in Figure 3.

	Black Oil
Ratio = 100.00 [%]	100.00
Sorption [g/gKerC]	0
Frequency factor [1e+25/Ma]	116.00
Activation energy [kcal/mol]	Fractions [%]
43.00	0.34
44.00	0.18
45.00	1.75
46.00	1.40
47.00	6.85
48.00	6.86
49.00	18.58
50.00	20.60
51.00	17.93
52.00	14.65
53.00	7.23
54.00	1.21
55.00	1.39
56.00	0.07
57.00	0.61
58.00	0.35
Σ	100.00

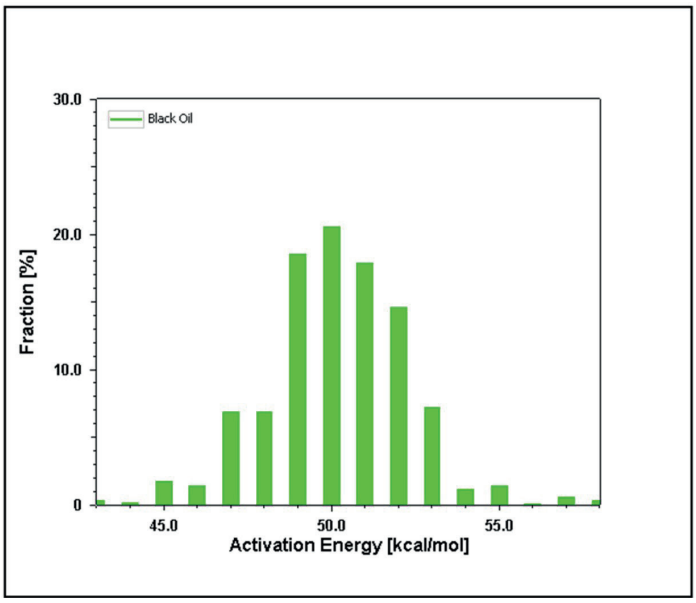

Fig. 3. *Mass (single component) kinetic model of kerogen for analyzed sample*

Py-GC analysis

Py-GC analyses show that the proportion of individual fractions changes in successive stages of pyrolysis (with increasing temperature). In the temperature range of 400–475°C, the share of the liquid hydrocarbon fraction in pyrolysis products exceeds 80%, while the share of the gaseous fraction (C_1–C_5) ranges from over 13% to almost 19%. In contrast, at higher temperatures, the proportion of the gaseous fraction increases rapidly. At 500°C it is 40%, at 525°C it reaches almost 75%, and at higher temperatures (500–700°C) it reaches 100% (Table 2). These results confirm that under natural geological conditions the composition of generated hydrocarbons also changes with the temperature of the source rock and the degree of thermal transformation of the kerogen. It also justifies the need for constructing and usage of multicomponent kerogen models for modeling petroleum systems, as well as the dynamics of generation process and the proportions of the generated fractions which change with the degree of thermal transformation of source rocks. The results of the analyses are presented in Table 2 and Figure 4.

Table 2
Results of multi-stage pyrolysis (Py-GC) of sample No. 1

Temperature [°C]	Fraction of products [%]	Proportion of pyrolytic fractions [%]				Proportion of pyrolytic fractions in total [%]		
		C_1–C_5	C_6–C_{14}	C_{15+}	Sum	C_1–C_5	C_6–C_{14}	C_{15+}
400	3.47	18.82	38.81	42.37	100.00	0.65	1.35	1.47
425	4.98	13.04	42.20	44.76	100.00	0.65	2.10	2.23
450	12.13	15.23	50.90	33.87	100.00	1.85	6.17	4.11
475	13.77	16.91	49.81	33.28	100.00	2.33	6.86	4.58
500	40.20	40.51	44.45	15.04	100.00	16.29	17.87	6.05
525	14.96	74.48	24.42	1.10	100.00	11.14	3.65	0.16
550	2.15	100.00	0.00	0.00	100.00	2.15	0.00	0.00
600	3.39	100.00	0.00	0.00	100.00	3.39	0.00	0.00
700	4.95	100.00	0.00	0.00	100.00	4.95	0.00	0.00
800	0.00	0.00	0.00	0.00	0.00	0.00	0.00	0.00
Fractional share of total [%]	Σ 100.00					Σ 43.40	Σ 38.00	Σ 18.60

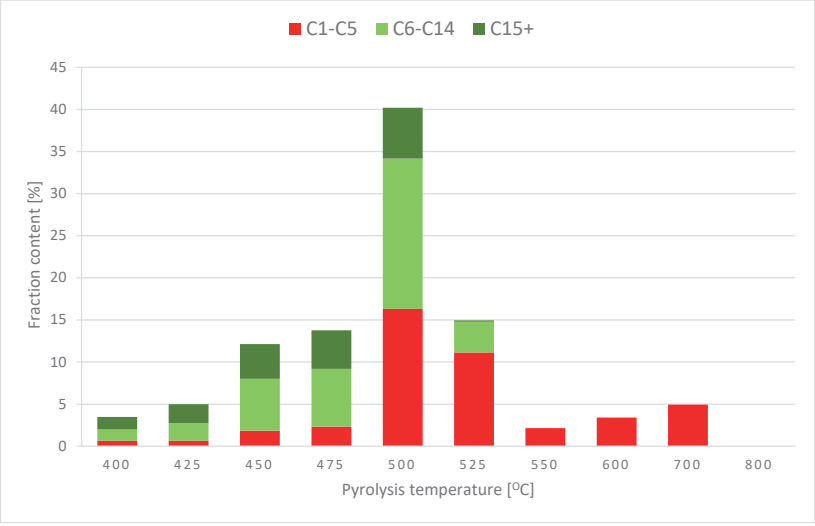

Fig. 4. *Proportion of hydrocarbon fractions in multi-stage pyrolysis products (Py-GC)*

The adopted concept for the calculation of activation energy distribution of the three-component kinetic model of kerogen

The mass (one-component) kinetic model and the results of multi-stage pyrolysis Py-GC formed the basis for the construction of a multi-component kinetic model.

Constructing multi-component kinetic models is a challenging task, mainly due to the inability to record the *k*-reaction rate for each of the pyrolysis products separately. However, the *k*-reaction rate can be realized by integrating the mass (one-component) model with the results of the multi-stage pyrolysis Py-GC. With a great simplification, it can be assumed that the activation energy of a compound (a component of kerogen) is proportional to the temperature at which its cracking takes place. Thus, in the first stage of pyrolysis, the kerogen compounds with the lowest chemical bond energy are cracked, and in each subsequent stage, the compounds with higher and higher energy, until the compounds with the highest bond energy (the highest activation energy), are completely cracked in the last stage of pyrolysis (the highest temperature). Taking into account the law of conservation of mass, it is possible to quantitatively assign the products of each stage of pyrolysis (the content of individual fractions) to the parts of kerogen with the appropriate activation energy, the distribution of which has been calculated in the mass model.

The basis for the construction of the multicomponent model is the one-component kinetic model (Fig. 3) of kerogen developed for sample No. 1, which is defined by the Arrhenius constant and the calculated activation energy distribution.

The method proposed by the authors consists of calculating the discrete distribution of activation energy for individual fractions, with a constant value of the preexponential factor *A* (Arrhenius constant), the value of which has been optimized for the mass model in the Kinetics15. Construction of the three-component model was based on the integration of a single-component (mass) model (Fig. 3, Table 3) with the results of multi-stage Py-GC pyrolysis (Table 2).

The method of calculating the activation energy distribution for the three-component model is presented below. For a better understanding of the calculation scheme proposed by the authors, its description should be confronted with the results in Table 3. It correlates the results of multi-stage pyrolysis with the activation energy distribution of the single-component kinetic model of kerogen. The calculations take into account the law of conservation of mass, according to which the percentage of hydrocarbons formed during each pyrolysis step by cracking kerogen is equal to the percentage of the kerogen's hydrocarbon potential that has been depleted. With great simplification, it can be assumed that in each of the successive stages of pyrolysis of Py-GC, (at stepwise increased temperature) kerogen with increasingly higher activation energy was cracked. The proportions of the different fractions in each stage of pyrolysis, and therefore kerogen with different activation energies were different. A comparison of the results of multi-stage PY-GC pyrolysis with the activation energy distribution of the single-component model (Table 3) for the studied sample reveals that during certain stages of PY-GC pyrolysis, kerogen with a wide range of activation energies is cracked (e.g., stage I – kerogen with an activation energy of 43–46 kcal/mol, stage V – kerogen with an activation energy of 49–52 kcal/mol, or stage IX – kerogen with an activation energy of 53–58 kcal/mol). Meanwhile, kerogen with a narrow activation energy range, such as 49 kcal/mol, spans three stages of PY-GC pyrolysis (stages III, IV, and V), and kerogen with an activation energy of 53 kcal/mol extends from stage VI to stage IX.

The products of the first stage of Py-GC pyrolysis (400°C) account for 3.47% of the hydrocarbons formed during all pyrolysis stages combined (Table 2). Based on the distribution of kerogen activation energy derived from the mass model, it can be assumed that this amount (3.47%) "depletes" kerogen with activation energy in the range of 43, 44, 45 kcal/mol (0.33% + 0.18% + 1.75%), and partially 46 kcal/mol (1.21%) (Table 3). However, the proportion of hydrocarbons formed by cracking kerogen with an activation energy of 46 kcal/mol is 1.41%, so it was assumed that the missing 0.2% was formed during

the second stage of PY-GC pyrolysis. A total of 4.98% of hydrocarbons were formed during the second stage, so it can be assumed that the remaining 4.78% is a product of kerogen cracking with an activation energy of 47 kcal/mol. The total amount of kerogen cracking products with an activation energy of 47 kcal/mol is 6.85%, so the missing 2.07% was assumed to have undergone cracking during the third stage (450°C). The products of the third pyrolysis stage account for a total of 12.10% of the total hydrocarbons, of which 2.07% are from kerogen with an activation energy of 47 kcal/mol, 6.86% with an activation energy of 48 kcal/mol, and 3.17% with an activation energy of 49 kcal/mol. The remainder of the kerogen with an activation energy of 49 kcal/mol was pyrolyzed in the fourth stage at 475°C (13.77%) and in the fifth stage at 500°C (1.62%). In the fifth pyrolysis stage, a total of 40.20% of the organic matter underwent cracking. In addition to 1.62% that was kerogen with an activation energy of 49 kcal/mol, 20.60% was kerogen with an activation energy of 50 kcal/mol, 17.90% with 51 kcal/mol, and 0.02% with an activation energy of 52 kcal/mol. The subsequent pyrolysis step (525°C) produced 14.96% hydrocarbons, of which 14.63% was from kerogen with an activation energy of 52 kcal/mol, and the remainder (0.33%) from kerogen with an activation energy of 53 kcal/mol. In addition, kerogen with an activation energy of 53 kcal/mol underwent cracking in the following pyrolysis stages: 2.15% at 550°C, 3.39% at 600°C and 1.35% at 700°C. A total of 4.95% of the total hydrocarbons were formed at 700°C, including 1.19% from kerogen with an activation energy of 54 kcal/mol, 1.39% with 55 kcal/mol, 0.07% with 56 kcal/mol, 0.61% with 57 kcal/mol and 0.35% with an activation energy of 58 kcal/mol (Table 3).

The construction of the multicomponent model involved calculating the absolute percentages of each hydrocarbon fraction for each discrete activation energy value (derived from the single-component model) across its range.

For example, the absolute percentage of the C_1–C_5 fraction for kerogen with an activation energy of 43 kcal/mol relative to the total hydrocarbon potential is 18.82% of 0.33%, which is equal to 0.06% of the total pyrolysis products. The percentages of all hydrocarbon fractions were calculated identically for kerogen with other discrete activation energy values, which was completely pyrolyzed during only one of the pyrolysis stages. Based on the absolute percentages of each fraction corresponding to specific discrete activation energy values of the kerogen, the quantitative proportions of each hydrocarbon fraction were also calculated (Table 3).

In the case of kerogen with a specific discrete activation energy value whose pyrolysis spanned more than one stage (for kerogen with discrete values of 46, 47, 49, 52, 53 kcal/mol), their absolute percentages in each pyrolysis stage had to be calculated and then summed. For example, for kerogen with a discrete activation energy value of 49 kcal/mol, whose pyrolysis occurred during the third, fourth and fifth stages, the proportions of each fraction are as follows: for the C_1–C_5 fraction it is 3.48% (0.49% from stage III + 2.33% from stage IV + 0.66% from stage V), for the C_6–C_{14} fraction it is 9.2% (1.63% + 6.86% + 0.71%, respectively) and for the C_{15+} fraction it is 5.91% (1.08% + 4.58% + 0.25%, respectively). According to the above scheme, the absolute percentages of each fraction were calculated for the remaining kerogen with specific discrete activation energy values (46, 47, 52, 53 kcal/mol), which was pyrolyzed during more than one step (Table 3). The parameters of the kinetic model developed for the kerogen of Menilite Beds and the visualization of the distribution of kerogen activation energy are shown in Table 4 and Figure 5.

The synthesis of results obtained from both methods proves that the proportion of individual hydrocarbon fractions generated during artificial maturation changes with increasing temperature. This indicates that the composition of hydrocarbons generated during the progressive thermal transformation of the source rock under natural geological conditions changes, and at each stage, the proportion of the generated hydrocarbon fractions may vary.

The thermal cracking of kerogen produces both liquid and gaseous hydrocarbons. However, as the thermal regime and the degree of thermal transformation of kerogen increase, the dynamics of the hydrocarbon generation process and the molecular composition of the produced hydrocarbons changes.

Table 3

Scheme of the procedure for calculating activation energy distribution of multi-component kinetic models of kerogen

Mass model			Py-GC results						Three-component model		
Activation energy [kcal/mol]	Fraction [%]		Stage/ Tempeature [°C]	Fraction of products [%]	Proportion of each fraction in each pyrolysis stage [%]				Fraction [%]		
					Σ	C_1–C_5	C_6–C_{14}	C_{15+}	C_1–C_5	C_6–C_{14}	C_{15+}
43	0.33	0.33	I/400	3.47	100.00	18.80	38.80	42.40	0.06	0.13	0.14
44	0.18	0.18							0.03	0.07	0.08
45	1.75	1.75							0.33	0.68	0.74
46	1.41	1.21							0.26	0.55	0.60
		0.20	II/425	4.98	100.00	13.0	42.20	44.80			
47	6.85	4.78							0.94	3.07	2.84
		2.07	III/450	12.13	100.00	15.20	50.90	33.90			
48	6.86	6.86							1.04	3.49	2.33
49	18.59	3.20							3.48	9.20	5.91
		13.77	IV/475	13.77	100.00	16.90	49.80	33.30			
		1.62	V/500	40.20	100.00	40.40	44.60	15.00			
50	20.62	20.62							8.33	9.20	3.09
51	17.93	17.93							7.25	8.00	2.68
52	14.65	0.06							10.92	3.54	0.19
		14.63	VI/525	14.96	100.00	74.50	24.40	1.10			
53	7.22	0.33							7.15	0.07	0.00
		2.15	VII/550	2.15	100.00	100.00	0.00	0.00			
		3.39	VIII/600	3.39	100.00	100.00	0.00	0.00			
		1.35	IX/700	4.95	100.00	100.00	0.00	0.00			
54	1.19	1.19							1.19	0.00	0.00
55	1.39	1.39							1.39	0.00	0.00
56	0.07	0.07							0.07	0.00	0.00
57	0.61	0.61							0.61	0.00	0.00
58	0.35	0.35							0.35	0.00	0.00
Σ	100.00	100.00	Σ	100.00		43.40	38.00	18.60	43.40	38.00	18.60

Table 4
Parameters of the developed kinetic model of kerogen of Menilite Beds

Ratio = 354.00 mg HC/g TOC	153.6	134.5	65.9
Ratio = 100%	43.4	38.0	18.6
Frequency factor [1e+25/Ma]	116	116	116
Activation energy [kcal/mol]	**C_1–C_5 fractions [%]**	**C_6–C_{14} fractions [%]**	**C_{15+} fractions [%]**
43	0.06	0.13	0.14
44	0.03	0.07	0.08
45	0.33	0.68	0.74
46	0.26	0.55	0.6
47	0.94	3.07	2.84
48	1.04	3.49	2.33
49	3.48	9.20	5.91
50	8.33	9.20	3.09
51	7.25	8.00	2.68
52	10.92	3.54	0.19
53	7.15	0.07	0
54	1.19	0	0
55	1.39	0	0
56	0.07	0	0
57	0.61	0	0
58	0.35	0	0
	Σ 43.40	Σ 38.00	Σ 18.60

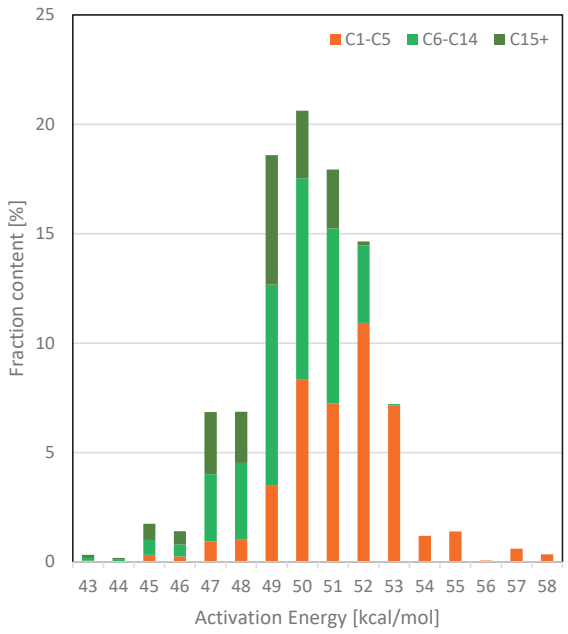

Fig. 5. *Visualization of the activation energy distribution of the developed kinetic model of kerogen from the Menilite Beds*

In general, at the initial stages of the thermal transformation of kerogen, hydrocarbons with a large number of carbon atoms in the molecule predominate, and as the degree of thermal transformation increases, the proportion of hydrocarbons with a smaller number of carbon atoms in the molecule increases; at the most advanced stage, practically only methane is produced. However, depending on the specificity of the source rock (maceral composition of the organic matter), the temperature at which the hydrocarbon generation process is initiated, as well as the dynamics of the process, and the composition of the generated hydrocarbons, in the same thermal regime for different source rocks, can vary greatly. As a consequence, implementing a random kinetic model of kerogen (one of the ones offered in the petroleum system modeling software) into the petroleum system model creates the risk of obtaining results with associated high inaccuracy.

In addition, simulations of the developed kinetic model showed significant differences in the proportions of individual hydrocarbon fractions for different degrees of thermal transformation (Fig. 6). At 40% transformation (Fig.6A), most of the hydrocarbons produced are in the C_6–C_{14} fraction, which is about twice as much as the C_1–C_5 fraction, while the amount of the C_{15+} fraction is intermediate. As the thermal transformation of kerogen increases, the proportion of lighter fractions increases. At 70% transformation, the C_6–C_{14} fraction accounts for about 45% of the total, the C_1–C_5 fraction for about one-third, and the C_{15+} fraction for the remainder (Fig. 6B). When the initial hydrocarbon potential is fully realised, the C_1–C_5 fraction will account for more than 43%, the C_6–C_{14} fraction will account for 38%, and the C_{15+} fraction will account for more than 18% (Fig. 6C).

The presented results, in the authors' opinion, sufficiently justify the rationale for constructing and implementing multi-component kinetic models of kerogen for the source rocks of the analyzed petroleum systems.

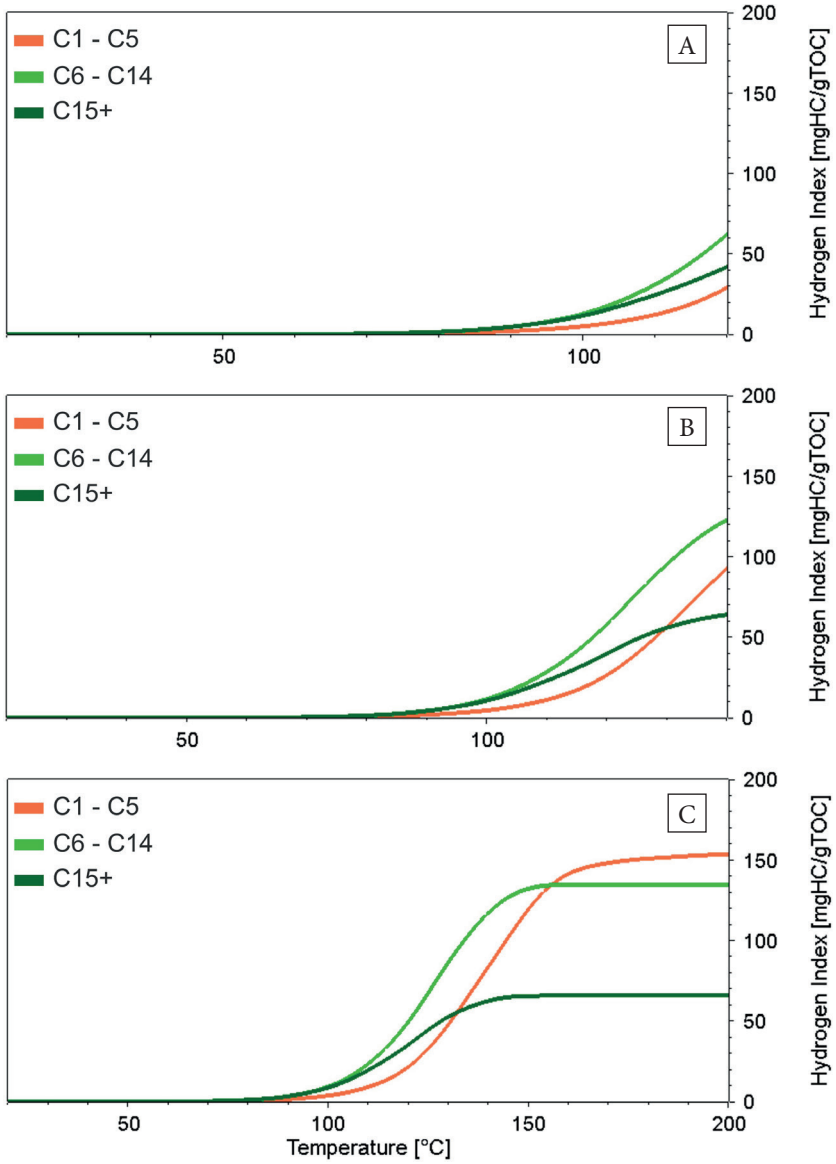

Fig. 6. *Variability in the shares of individual hydrocarbon fractions generated, based on the degree of thermal transformation (TR) of kerogen from the Menilite Beds, calculated using the kinetic model developed for the selected sample (No. 1): A) TR = 40%; B) TR = 70%; C) TR = 100%*

DISCUSSION

The results of comparative simulations conducted on kinetic models of kerogen developed for source rocks from various petroleum basins show that the degree of thermal transformation of the kerogen under identical thermal conditions varies significantly. For example, with a temperature increase from 20 to 120°C at a rate of 2°C/Ma, the thermal transformation coefficient of Type II kerogen differs considerably, ranging from a few percent for models such as Abu-Ali(1999)_TIIQusaiba and Dieckman(2000)_TII(WestCanadaB), to 33% for the Quiglay_et_al(1987)_TII model and 55% for the Behar_et_al(1997)_TII-(MontSh) model. Most commonly, it ranges 12–18%, as seen in models such as Behar_et_al(1997)_TII(PB), Vandenbroucke_et_al(1999)_TII(NorthSea), Dieckman(1998)_TII(LowSaxonianB), and Burnham(1989)_TII. For the model developed for the Menilite_Shales_(SilesianUnit), it is 45%. This indicates that kerogen from source rocks with the same initial hydrocarbon potential (the same hydrogen index, HI), when subjected to the same thermal regime, undergoes cracking to varying degrees, resulting in different generation efficiencies. For comparison, in the simulations, an identical hydrogen index (HI) value of 354 mg HC/g TOC, corresponding to the value measured for the kerogen in the analyzed sample, was assumed for each model. The efficiencies, corresponding to the degree of transformation, vary with increasing temperature, depending on the kinetic parameters of the kerogen. These changes are most easily observed using the Burnham(1989)_TII model as an example. For this model, the degree of kerogen transformation during a temperature increase from 20 to 120°C at a rate of 2°C/Ma reaches one of the lowest values among the compared models, amounting to only about 18% (Fig. 7). In contrast, under a higher thermal regime (temperature increase from 20 to 150°C at a rate of 2.6°C/Ma), the degree of transformation is the highest, reaching 95% (Fig. 8).

Moreover, the amount of generated hydrocarbons, both gaseous and liquid, as well as the ratios between these amounts, change with increasing temperature depending on the chosen model. For the model developed by the authors, Menilite_Shales_(SilesianUnit), at a temperature of 120°C with a rate of 2°C/Ma, the amount of the gaseous fraction exceeds 30 mg HC/g TOC, and the liquid fraction exceeds 110 mg HC/g TOC. In the same thermal regime, for the Burnham(1989)_TII model, the amounts are approximately 10 mg HC/g TOC and over 40 mg HC/g TOC, respectively (Fig. 9).

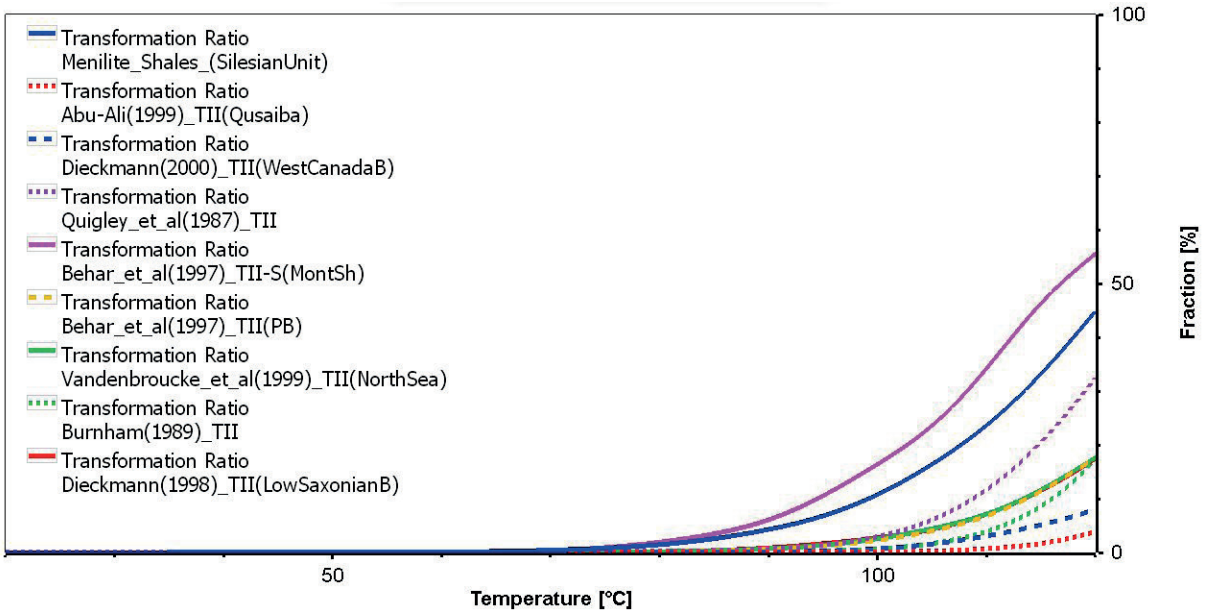

Fig. 7. *Transformation ratio (TR) (realization of initial hydrocarbon potential) of Type II kerogen for a temperature interval of 20–120°C at a rate of 2°C/Ma, depending on the kinetic model*

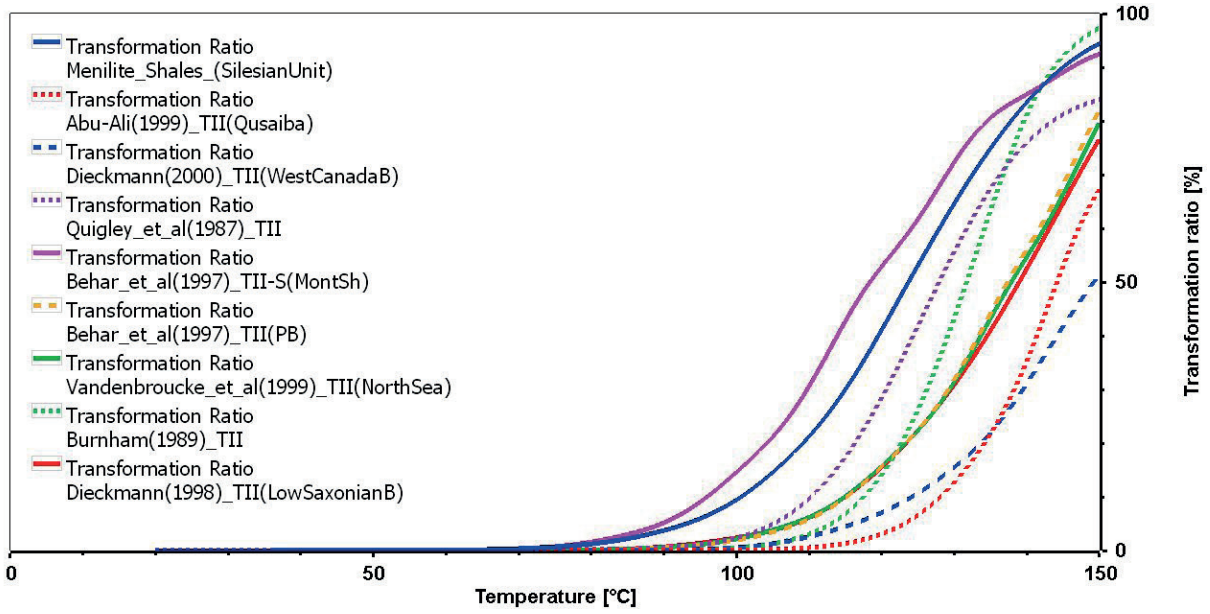

Fig. 8. *Transformation ratio (TR) (realization of initial hydrocarbon potential) of Type II kerogen for a temperature interval of 20–150°C at a rate of 2.6°C/Ma, depending on the kinetic model*

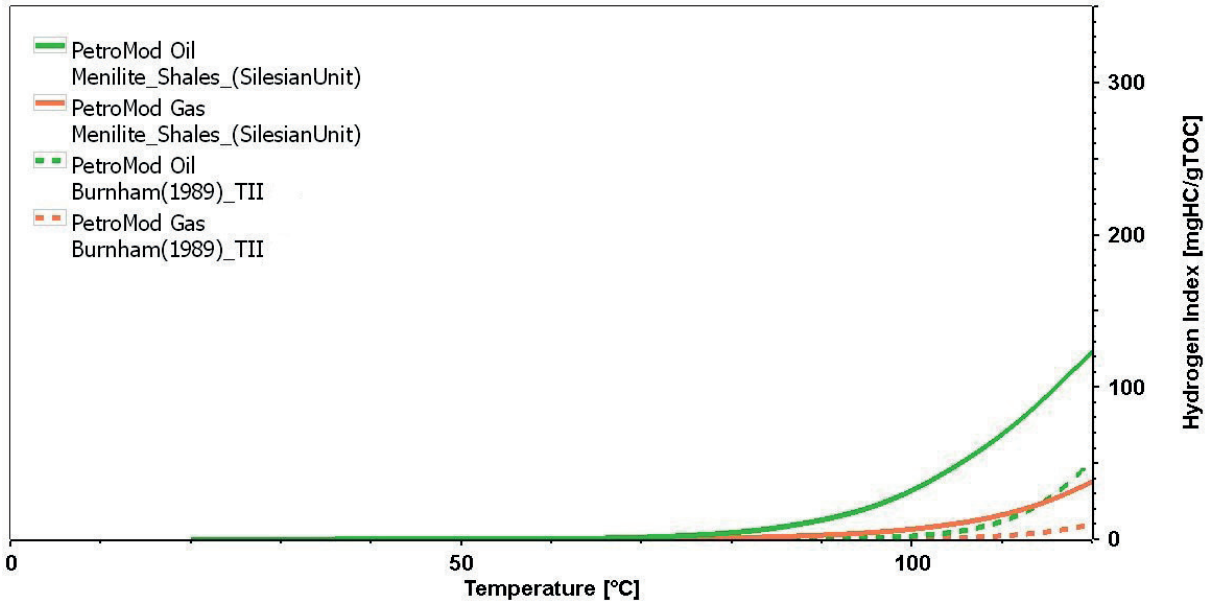

Fig. 9. *Hydrocarbon generation efficiency curves for liquid and gaseous fractions in the temperature range of 20–120°C at a rate of 2°C/Ma for the models: Menilite_Shales_(SilesianUnit) and Burnham(1989)_TII*

For the Menilite_Shales_(SilesianUnit) model, increasing the temperature to 150°C at a rate of 2.6°C/Ma results in the liquid fraction rising to 190 mg HC/g TOC and the gaseous fraction to over 130 mg HC/g TOC, indicating over 90% realization of the initial hydrocarbon potential. In the same thermal regime, for the Burnham(1989)_TII model, the liquid fraction increases to nearly 290 mg HC/g TOC, and the gaseous fraction to over 50 mg HC/g TOC (Fig. 10).

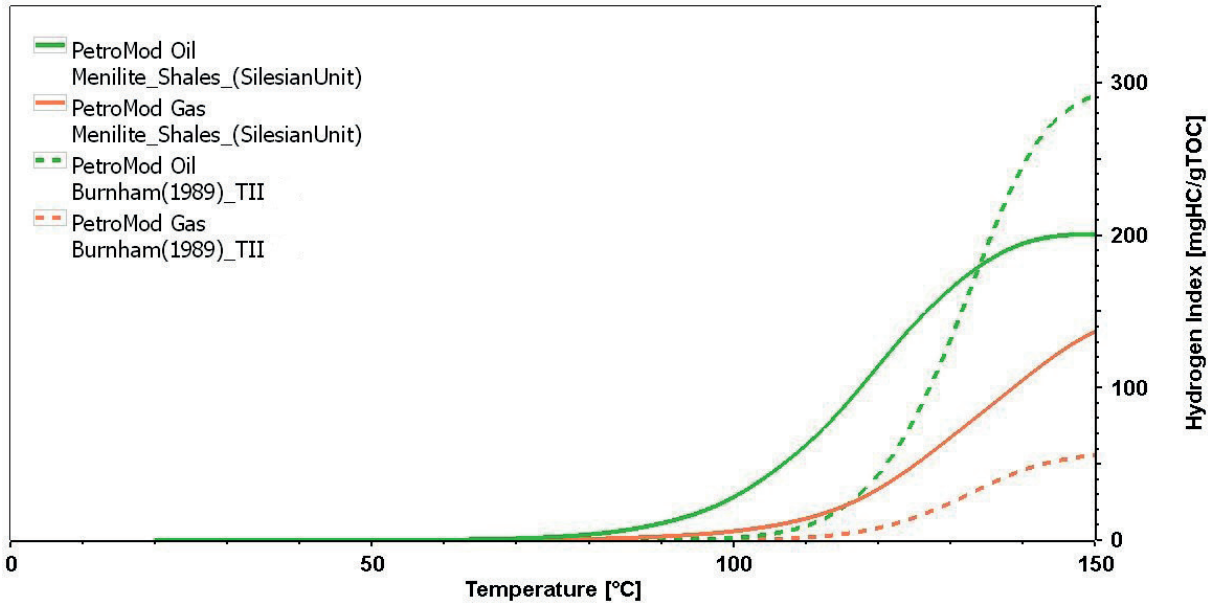

Fig. 10. *Hydrocarbon generation efficiency curves for liquid and gaseous fractions in the temperature range of 20–150°C at a rate of 2.6°C/Ma for the models: Menilite_Shales_(SilesianUnit) and Burnham(1989)_TII*

It should be noted that the temperature increase from 120 to 150°C causes nearly a sevenfold increase in the amount of generated liquid hydrocarbons for the Burnham(1989)_TII model, resulting in a value approximately 100 mg HC/g TOC higher than for the Menilite_Shales_(SilesianUnit) model, where the amount only nearly doubles. For the gaseous fraction, the quantitative proportions are different. For the Menilite_Shales_(SilesianUnit) model, there is about a fourfold increase, while for the Burnham(1989)_TII model, the increase is nearly sevenfold.

CONCLUSIONS

The developed procedure for calculating the parameters of the thermal decomposition of kerogen, on the example of selected samples of Menilite source rocks, showed that the application of a multicomponent kinetic model to simulate petroleum processes allows the precise assessment of the composition of generated hydrocarbons during thermal transformation.

Such a scheme, based on the integration of easily available analytical techniques (Rock-Eval and Py-GC), will enable the implementation of parameters characterizing the elements of the analyzed petroleum system into the PetroMod Kinetics Editor. This justifies the desirability of the adopted concept of creating multi-component kinetic models of kerogen. The methodological approach seems to be universal and can be used in further research studies of petroleum systems in Poland to build Poland's specific database of kerogen kinetics of hydrocarbon source rocks in analyzed petroleum basins. The methodology used to date for the assessment of kinetic parameters in the Kinetics15 program, based on the results of Rock-Eval pyrolysis, allowed us to determine the distribution of activation energy in terms of total hydrocarbon production, which is a significant simplification. The quantitative distribution of the generated hydrocarbons into individual fractions over time will enable the creation of the reliable modeling of petroleum systems in terms of time, space and the type of expected accumulations.

This paper was written on the basis of the statutory work entitled "Opracowanie metodyki konstrukcji wielokomponentowych modeli kinetycznych kerogenu" – the work of the Oil and Gas Institute – National Research Institute which was commissioned by the Ministry of Science and Higher Education; order number: 55/SG/22, archive number: SG-4101-43/22.

REFERENCES

Abu-Ali M.A., Rudkiewicz J.L., McGillivray J.G. & Behar F., 1999. Paleozoic petroleum system of Central Saudi Arabia. *GeoArabia*, 4(3), 321–336. https://doi.org/10.2113/geoarabia0403321.

Baur F., 2019. Predicting petroleum gravity with basin modeling: New kinetic models. *AAPG Bulletin*, 103(8), 1811–1837. https://doi.org/10.1306/12191818064.

Behar F., Vandenbroucke M., Tang Y., Marquis F. & Espitalie J., 1997. Thermal cracking of kerogen in open and closed systems: Determination of kinetic parameters and stochiometric coefficients for oil and gas generation. *Organic Geochemistry*, 26(5–6), 321–339. https://doi.org/10.1016/S0146-6380(97)00014-4.

Bordenave M.L., 1993. *Applied Petroleum Geochemistry*. Editions Technip, Paris.

Burnham A.K., 2017. *Global Chemical Kinetics of Fossil Fuels: How to Model Maturation and Pyrolysis*. Springer, Cham. https://doi.org/10.1007/978-3-319-49634-4.

Burnham A.K. & Braun R.L., 1990. Development of a detailed model of petroleum formation, destruction, and expulsion from lacustrine and marine source rocks. *Organic Geochemistry*, 16(1–3), 27–39. https://doi.org/10.1016/0146-6380(90)90023-S.

Burnham A.K. & Sweeney J.J., 1989. A chemical kinetic model of vitrinite maturation and reflectance. *Geochimica et Cosmochimica Acta*, 53, 2649–2657. https://doi.org/10.1016/0016-7037(89)90136-1.

Dieckmann V., Schenk H.J., Horsfield B. & Welte D.H., 1998. Kinetics of petroleum generation and cracking by programmed-temperature closed-system pyrolysis of Toarcian Shales. *Fuel*, 77(1–2), 23–31. https://doi.org/10.1016/S0016-2361(97)00165-8.

Dieckmann V., Horsfield B. & Schenk H.J., 2000. Heating rate dependency of petroleum-forming reactions: Implications for compositional kinetic predictions. *Organic Geochemistry*, 31(12), 1333–1348. https://doi.org/10.1016/S0146-6380(00)00105-4.

Dziadzio P., Matyasik I., Garecka M. & Szydło A., 2016. *Lower Oligocene Menilite Beds, Polish Outer Carpathians: Supposed deep-sea flysch locally reinterpreted as shelfal, based on new sedimentological, micropaleontological and organic-geochemical data*. Prace Naukowe Instytutu Nafty i Gazu Państwowego Instytutu Badawczego, 213, Instytut Nafty i Gazu – Państwowy Instytut Badawczy, Kraków. https://doi.org/10.18668/PN2016.213.

Espitalié J., Marquis F. & Barsony I., 1984. Geochemical logging. [in:] Voorhess K.J. (ed.), *Analytical Pyrolysis*, Butterworths, Boston, 53–79.

Espitalié J., Deroo G. & Marquis F., 1985. La pyrolyse Rock-Eval et ses applications. Deuxième partie. *Revue de l'Institut Français du Pétrole*, 40(6), 755–784. https://doi.org/10.2516/ogst:1985045.

Espitalié J., Ungerer P., Irwin I. & Marquis F., 1988. Primary cracking of kerogens. Experimenting and modeling C1, C2–C5, C6–C15 and C15+ classes of hydrocarbons formed. *Advances in Organic Geochemistry*, 13(4–6), 893–899. https://doi.org/10.1016/0146-6380(88)90243-4.

Hantschel T. & Kauerauf A., 2009. *Fundamentals of Basin and Petroleum Systems Modeling*. Springer, Berlin, Heidelberg. https://doi.org/10.1007/978-3-540-72318-9.

Hunt J.M., 1979. *Petroleum Geochemistry and Geology*. Freeman and Co., San Francisco.

Kania M. & Janiga M., 2015. Wykorzystanie pirolitycznej chromatografii gazowej do określania składu produktów symulowanego procesu generowania węglowodorów. *Nafta-Gaz*, 71(10), 720–728. https://doi.org/10.18668/NG.2015.10.02.

Krevelen D.W., van, 1961. *Coal: Typology – Chemistry – Physics – Constitution*. Coal Science and Technology Series, 3, Elsevier.

Lafargue E., Marquis F. & Pillot D., 1998. Rock-Eval 6 applications in hydrocarbon exploration, production and in soil contamination studies. *Oil & Gas Science and Technology*, 53(4), 421–437. https://doi.org/10.2516/ogst:1998036.

Lewan M.D. & Ruble T.E., 2002. Comparison of petroleum generation kinetics by isothermal hydrous and non-isothermal open-system pyrolysis. *Organic Geochemistry*, 33(12), 1457–1475. https://doi.org/10.1016/S0146-6380(02)00182-1.

Matyasik I. & Dziadzio P.S., 2006. Reconstruction of petroleum system based on integrated geochemical and geological investigation: Selected examples from middle Outer Carpathians in Poland. [in:] Golonka J. & Picha F.J. (eds.), *The Carpathians and Their Foreland: Geology and Hydrocarbon Resources*, AAPG Memoir, 84, American Association of Petroleum Geologists, Tulsa, 497–518. https://doi.org/10.1306/985618M843076.

Matyasik I. & Kupisz L., 1996. Geologiczno-geochemiczne uwarunkowania generacyjne warstw menilitowych depresji strzyżowskiej. *Nafta-Gaz*, 52(11), 469–479.

Pepper A.S. & Corvi P.J., 1995. Simple kinetic models of petroleum formation. Part I: oil and gas generation from kerogen. *Marine and Petroleum Geology,* 12(3), 291–319.

Quigley T.M., Mackenzie A.S. & Gray J.R., 1987. Kinetic theory of petroleum generation. [in:] Doligez B. (ed.), *Migration of Hydrocarbons in Sedimentary Basins: 2nd IFP Exploration Research Conference, Carcans, France, June 15–19, 1987*, Editions Technip, Paris, 649–666.

Santamaria-Orozco D.M., 2000. *Organic Geochemistry of Tithonian Source Rocks and Associated Oils from the Sonda de Campeche, Mexico*. Berichte des Forschungszentrums Jülich, 3763, Forschungszentrum, Zentralbibliothek, Jülich.

Sowiżdżał K., Słoczyński T., Sowiżdżał A., Papiernik B. & Machowski G., 2020. Miocene Biogas Generation System in the Carpathian Foredeep (SE Poland): A Basin Modeling Study to Assess the Potential of Unconventional Mudstone Reservoirs. *Energies*, 13(7), 1–26. https://doi.org/10.3390/en13071838.

Spunda K., 2020. Modelowanie 1D procesów generowania węglowodorów z warstw istebniańskich w profilu odwiertu nawiercającego utwory jednostki śląskiej. *Nafta-Gaz*, 76(2), 57–75. https://doi.org/10.18668/NG.2020.02.01.

Spunda K. & Słoczyński T., 2022. Energia aktywacji utworów warstw menilitowych i jej implikacje dla procesu generowania węglowodorów w Karpatach. *Nafta-Gaz*, 78(5), 327–335. https://doi.org/10.18668/NG.2022.05.01.

Spunda K., Słoczyński T. & Sowiżdżał K., 2021. Ocena wpływu nasuwającego się górotworu karpackiego na przebieg procesów naftowych w utworach jego podłoża w rejonie Rzeszowa. *Nafta-Gaz*, 77(6), 351–365. https://doi.org/10.18668/NG.2021.06.01.

Sweeney J.J. & Burnham A.K., 1990. Evaluation of a simple model of vitrinite reflectance based on chemical kinetics. *AAPG Bulletin*, 74(10), 1559–1570. https://doi.org/10.1306/0C9B251F-1710-11D7-8645000102C1865D.

Tegelaar E.W. & Noble R.A., 1994. Kinetics of hydrocarbon generation as a function of the molecular structure of kerogen as revealed by pyrolysis-gas chromatography. *Organic Geochemistry*, 22(3–5), 543–574. https://doi.org/10.1016/0146-6380(94)90125-2.

Ungerer P., 1990. State of the art of research in kinetic modelling of oil formation and expulsion. *Organic Geochemistry,* 16(1–3), 1–25. https://doi.org/10.1016/0146-6380(90)90022-R.

Vandenbroucke M., Behar F. & Rudkiewicz J.L., 1999. Kinetic modelling of petroleum formation and cracking: implications from the high pressure/high temperature Elgin Field (UK, North Sea). *Organic Geochemistry*, 30(9), 1105–1125. https://doi.org/10.1016/S0146-6380(99)00089-3.

Waples D.W., Kamata H. & Suizu M., 1992. The art of maturity modeling. Part 2: Alternative models and sensitivity analysis. *AAPG Bulletin,* 76(1), 47–66.

Wood D.A., 2024. Kerogen kinetic distributions and simulations provide insights into petroleum transformation fraction (TF) profiles of organic-rich shales. *Journal of Earth Science*, 35(3), 747–757. https://doi.org/10.1007/s12583-024-1981-0.

Zhou Y. & Littke R., 1999. Numerical simulation of the thermal maturation, oil generation and migration in the Songliao Basin, Northeastern China. *Marine and Petroleum Geology*, 16(8), 771–792. https://doi.org/10.1016/S0264-8172(99)00043-4.